

# A reduction of mitochondrial DNA molecules during embryogenesis explains the rapid segregation of genotypes

Lynsey M Cree<sup>1</sup>, David C Samuels<sup>2</sup>, Susana Chuva de Sousa Lopes<sup>3</sup>, Harsha Karur Rajasimha<sup>2</sup>, Passorn Wonnapijit<sup>2</sup>, Jeffrey R Mann<sup>4,7</sup>, Hans-Henrik M Dahl<sup>5</sup> & Patrick F Chinnery<sup>1,6</sup>

**Mammalian mitochondrial DNA (mtDNA) is inherited principally down the maternal line, but the mechanisms involved are not fully understood. Females harboring a mixture of mutant and wild-type mtDNA (heteroplasmy) transmit a varying proportion of mutant mtDNA to their offspring. In humans with mtDNA disorders, the proportion of mutated mtDNA inherited from the mother correlates with disease severity<sup>1–4</sup>. Rapid changes in allele frequency can occur in a single generation<sup>5,6</sup>. This could be due to a marked reduction in the number of mtDNA molecules being transmitted from mother to offspring (the mitochondrial genetic bottleneck), to the partitioning of mtDNA into homoplasmic segregating units, or to the selection of a group of mtDNA molecules to repopulate the next generation. Here we show that the partitioning of mtDNA molecules into different cells before and after implantation, followed by the segregation of replicating mtDNA between proliferating primordial germ cells, is responsible for the different levels of heteroplasmy seen in the offspring of heteroplasmic female mice.**

Rapid changes in mitochondrial allele frequency were first observed in the offspring of Holstein cows<sup>5,6</sup>. Similar changes have subsequently been described in many mammalian species, including humans transmitting pathogenic mtDNA mutations<sup>1,3,4,7</sup>. In heteroplasmic mice transmitting neutral mtDNA polymorphisms, the percentage level of heteroplasmy seen in the offspring is determined at an early stage during oogenesis in the developing mother, before the formation of the primary oocytes<sup>8</sup>. The same process appears to explain the transmission of highly pathogenic mtDNA mutations<sup>9,10</sup>, present in ~1 in 5,000 of the population.

The size of the mitochondrial genetic bottleneck in mice is predicted to be ~200 segregating units<sup>8</sup>. Given that the total amount

of mtDNA remains constant within dividing preimplantation mouse embryos<sup>11</sup>, we initially determined whether the amount of mtDNA within single blastomeres fell to ~200 immediately before implantation at 5.5 days *post coitum* (d.p.c.; **Table 1**). The median number of mtDNA molecules in mature oocytes was  $2.28 \times 10^5$ , and the total amount of mtDNA within the entire preimplantation embryo remained constant ( $F = 1.82$ ,  $P = 0.101$ , **Fig. 1a**). These values are consistent with previous estimates<sup>11,12</sup> and confirm that mtDNA replication is not required for healthy preimplantation development<sup>13</sup>. With sequential binary cell divisions, the amount of mtDNA in each cell fell to an estimated value of ~4,000 mtDNA molecules immediately before implantation (**Fig. 1b, Table 1**), some ~20-fold greater than predicted<sup>8</sup>. We therefore concluded that the mtDNA genetic bottleneck is not due to subdivision of a non dividing mtDNA pool in the preimplantation embryo.

Primary oocytes are first detectable at 7.25 d.p.c. and develop from a founder population of 40 primordial germ cell (PGCs) recruited by induction from the epiblast in the posterior-proximal embryonic pole<sup>14</sup>. To determine whether the amount of mtDNA in PGCs could explain the mtDNA bottleneck, we studied fluorescently sorted PGCs from mice expressing green fluorescent protein–tagged Stella, which is the most specific marker of PGCs<sup>15</sup>. The first discernable PGCs contained substantially lower amounts of mtDNA than the preimplantation blastomeres (**Table 2**). PGCs isolated from embryos at 8.5–14.5 d.p.c. contained greater amounts of mtDNA, indicating that mtDNA replication had commenced (**Fig. 1c**), but the average amount of mtDNA within the developing PGCs remained ~100-fold lower than in mature oocytes (median mtDNA copies per PGC at 14.5 d.p.c., 1,529). The median number of mtDNA molecules present within 7.5–d.p.c. PGCs was 203, which closely approximates a previous estimate (185 segregating units<sup>8</sup>) inferred from heteroplasmic mice using a model based upon population genetic theory<sup>8,16</sup>.

<sup>1</sup>Mitochondrial Research Group, Newcastle University, Newcastle NE2 4HH, UK. <sup>2</sup>Virginia Bioinformatics Institute, Virginia Polytechnic Institute and State University, Blacksburg, Virginia 24061, USA. <sup>3</sup>Wellcome Trust/Cancer Research UK Gurdon Institute, University of Cambridge, Tennis Court Road, Cambridge CB2 1QN, UK. <sup>4</sup>Division of Biology, City of Hope, 1500 E. Duarte Rd., Duarte, California 91010, USA. <sup>5</sup>The Murdoch Children's Research Institute & Department of Paediatrics (University of Melbourne), Royal Children's Hospital, Parkville, Melbourne, Victoria 3052, Australia. <sup>6</sup>Institute of Human Genetics, Newcastle University, Newcastle NE2 4HH, UK. <sup>7</sup>Present address: Department of Zoology, The University of Melbourne, Victoria 3010, Australia. Correspondence should be addressed to P.F.C. (p.f.chinnery@ncl.ac.uk).

Received 16 April 2007; accepted 19 October 2007; published online 27 January 2008; doi:10.1038/ng.2007.63

**Table 1** Amount of mtDNA in mature oocytes and preimplantation mouse embryos

Stage	Whole embryo					Individual blastomeres				
	<i>n</i>	Mean copy number ( $\times 10^3$ )	Median copy number ( $\times 10^3$ )	Range ( $\times 10^3$ )	CV	<i>n</i>	Mean copy number ( $\times 10^3$ )	Median copy number ( $\times 10^3$ )	Range ( $\times 10^3$ )	CV
Oocyte	–	–	–	–	–	22	249.4	228.5	26.9–645.7	0.63
2 cell	24	347.7	312.8	112.9–676.8	0.54	18	247	245.3	14.6–465.6	0.52
4 cell	13	196	174.3	85.9–483.2	0.55	9	57.7	36.3	15.1–143.6	0.9
6 cell	8	308.6	287.8	150.5–547.6	0.41	19	63.2	47.1	20.4–166.0	0.6
8 cell	23	244.5	243.0	73.8–488.2	0.41	33	47.9	32.2	11.0–281.0	1.07
16–32 cell	12	286.1	267.7	73.8–671.3	0.52	11	18.4	15.4	4.9–38.0	0.61
Blastocyst	15	280.8	212.8	56.7–667.1	0.68	–	–	–	–	–

CV, coefficient of variance; *n*, number of cells studied.

Previous estimates of the mitochondrial genetic bottleneck are critically dependent upon the chosen mathematical model. A single-sampling binomial model describes the whole process and has been used to predict the chance of transmitting a particular level of heteroplasmy<sup>17,18</sup>, but it does not reflect the underlying biology (Fig. 2a). The population genetic model<sup>8,16</sup> assumes that the bottleneck occurs while numerous generations of cells are being formed by binary cell division, with each cell containing the same amount of mtDNA (Fig. 2b). For example, the bottleneck of ~185 segregating units was assumed to be present for 15 germ-cell divisions<sup>8</sup>, but our observations show that the amount of mtDNA within PGCs increases between 7.5 and 14.5 d.p.c. (Fig. 1c). We therefore adapted these models using the experimental data to model the biological process directly (Fig. 2c). Before implantation, the model was based on binary cell division of a heteroplasmic mouse embryo with no mtDNA replication, using experimentally determined values for the amount of mtDNA within single blastomeres (Table 1) and the rate of cell division<sup>19</sup>. After implantation, the model included mtDNA replication at the minimum rate required to populate the increasing number of PGCs<sup>20,21</sup>, and it was also based on experimentally determined values for the median amount of mtDNA within single PGCs (Table 2, Fig. 3a) and the rate of cell division required to produce 25,791 primary oocytes at day 13.5 (ref. 21) (Supplementary Figs. 1 and 2 online).

To determine whether the biological model reliably predicted the transmission of mtDNA heteroplasmy, we studied the transmission in 246 offspring from 22 litters born to mothers with different levels of NZB/C57BL/6J heteroplasmy generated by cytoplasm transfer (Supplementary Table 1 online). 91% of the offspring had NZB heteroplasmy levels that fell within the predicted 95% confidence interval (CI) for the model (Fig. 3b). The simulation results in Figure 3b are based on a conservative model using the median value for the number of mtDNA copies per cell at 7.5 d.p.c. However, when we simulated a 12-h delay in the onset of mtDNA replication, consistent with the observed variation in implantation time<sup>22</sup>, this led to a reduction in mtDNA copies at implantation that approximated the lower end of the measured range in *Stella-GFP* PGCs (Table 2) and to a greater variance in heteroplasmy values among the offspring.

Together, these observations indicate that the reduction in mtDNA copies we

observed during immediate preimplantation and postimplantation development is sufficient to generate the variation in heteroplasmy levels seen among the offspring of heteroplasmic female mice. Approximately 70% of the heteroplasmy variance was due to the physical partitioning of mtDNA molecules into daughter cells during pre- and early postimplantation development, when the amount of mtDNA in each cell fell to low levels (~200). The remaining ~30% developed during the intense proliferation of mtDNA in the exponentially expanding PGC population, where the average amount of mtDNA was ~1,500 molecules per PGC (Fig. 3a,c and Supplementary Fig. 2). Variation in heteroplasmy levels will occur without the compartmentalization of mtDNA molecules into multicopy segregating units such as nucleoids or mitochondria, or through the selection of particular group of mtDNAs chosen to repopulate the next generation.

Cao *et al.*<sup>23</sup> reported >1,000 mtDNA molecules in 7.5-d.p.c. PGCs and concluded that the mitochondrial genetic bottleneck is due not to a drastic decline in mtDNA copy number but to a small effective number of effective segregating units, each containing multiple mtDNA molecules. How can we explain the discrepancy between their findings and ours? Differences in our experimental approach explain why we measured a lower number of mtDNA molecules in early PGCs, and our interpretation of these data using a biologically plausible model led us to conclude that the mtDNA molecule is the segregating unit.

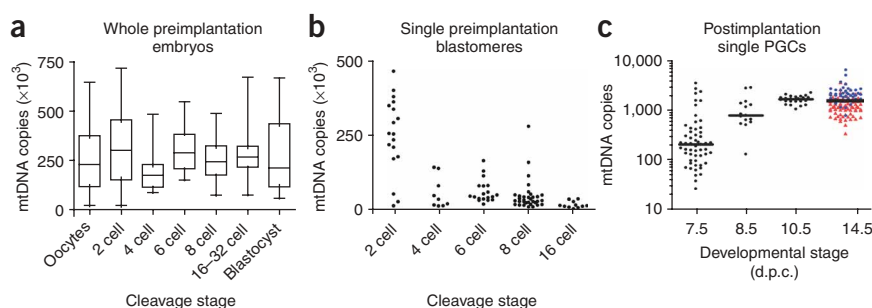


**Figure 1** The amount of mtDNA in mature mouse oocytes and preimplantation mouse embryos. (a) Mature oocytes and whole embryos. Box and whisker diagram showing the median,  $\pm 1$  s.d., and the range from maximum to minimum values. (b) Single blastocyst cells (blastomeres) from preimplantation embryos. Each data point corresponds to a single blastomere. (c) Primordial germ cells (PGCs) from postimplantation mouse embryos on a logarithmic plot. Each data point corresponds to a single PGC. Horizontal line indicates median value. Data from male and female embryos is shown separately for 14.5 d.p.c. Blue circles, males; red triangles, females.

**Table 2** Amount of mtDNA in primordial germ cells at different embryonic stages in mice

Stage	<i>n</i>	Mean copy number ( $\times 10^2$ )	Median copy number ( $\times 10^2$ )	Range ( $\times 10^3$ )	CV
7.5 d.p.c.	596	4.51	2.03	0.26–34.02	1.55
8.5 d.p.c.	165	10.65	7.68	1.28–27.78	0.72
10.5 d.p.c.	96	16.01	16.30	10.26–21.93	0.18
14.5 d.p.c., male	1,087	21.52	19.98	7.56–62.41	0.44
14.5 d.p.c., female	1,528	13.76	12.88	3.42–34.13	0.44

CV, coefficient of variance; *n*, number of primordial germ cells studied; d.p.c., days *post coitum*.

Before using *Stella-GFP* mice, we explored the possibility of using alkaline phosphatase histochemistry to identify PGCs. Like Cao *et al.*<sup>23</sup>, we found that the stain decreased the number of copies measured within individual cells. In our hands, the alkaline phosphatase histochemistry did not affect all cells equally, leading to an increased variability in copy number values. Light microscopy showed that the stain diffused out of PGCs in cryostat sections both at 37 °C and at room temperature, making it difficult to identify which cells were PGCs and which were not. This was particularly a problem when the PGC population was small at 7.5 d.p.c. The correction factor of 1.96 used by Cao *et al.*<sup>23</sup>, to compensate for the decreased efficiency of the real-time PCR reaction in alkaline phosphatase-stained cells, would not account for the increased variability that we observed. Moreover, as only 95% of alkaline phosphatase-positive PGCs express *Stella*<sup>15</sup>, it is generally accepted that *Stella-GFP* is the more accurate marker of the PGC lineage<sup>15</sup>. It is therefore possible that some of the alkaline phosphatase-stained cells analyzed by Cao *et al.*<sup>23</sup> were not actually PGCs. Using *Stella-GFP*-labeled mice, we reliably measured a ~7.5-fold lower number of mtDNA molecules in early PGCs.

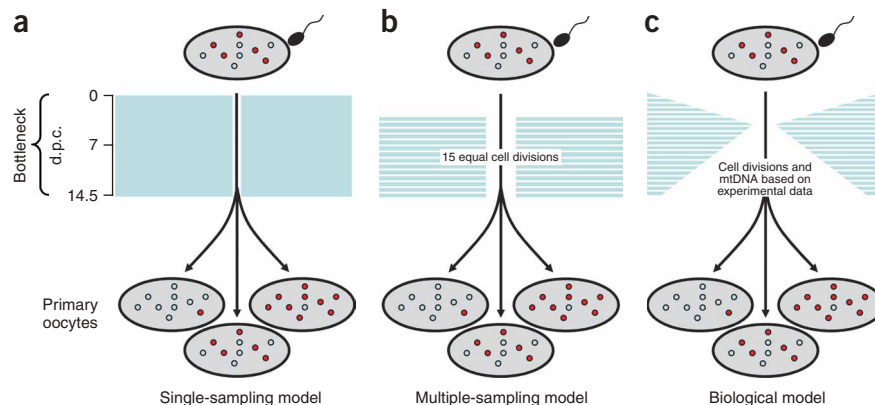
Finally, our interpretation of the data was based on a model that simulates the biological process directly, incorporating our laboratory data and what is known about the replication of mtDNA and the dynamics of cell division. Comparing the population genetic model<sup>8,16</sup> to our model during the linear phase (after 9 d.p.c.) shows that the relaxed replication of mtDNA contributes considerably to the variation in heteroplasmy levels, particularly during the rapid proliferation of mtDNA molecules in the expanding germ line. Using the model we describe here, the segregation of replicating mtDNA molecules generates sufficient variation in heteroplasmy levels to explain our

observations in heteroplasmic mice, indicating that the mtDNA molecule itself is the segregating unit during transmission. Additional variation could arise through the variation in copy number we observed in 7.5-d.p.c. PGCs. This could, in part, arise through differences in the time of implantation and the resumption of mtDNA replication or through uneven partitioning of mtDNA during cytokinesis. Although the time of implantation in the simulation model was set to reproduce the experimentally determined time course of

the median mtDNA copy number, other factors related to the observed variation in copy number between cells were not included in the model. Including these factors would only add weight to our conclusions.

Why is there a mitochondrial genetic bottleneck? mtDNA lacks protective histones and is close to the respiratory chain, a potent source of mutagenic free radicals. Mitochondria are also relatively deficient in DNA repair mechanisms, contributing to the mutation rate of mtDNA. The mitochondrial genetic bottleneck leads to the rapid segregation of new genotypes, which either are lost during transmission or reach very high levels and affect fecundity. This facilitates the rapid removal of deleterious mtDNA mutations from the population, by 'purifying' germline mtDNA, and thus prevents the 'mutational meltdown' predicted by Muller's ratchet<sup>24</sup>. This is not only important for the female germ line, but it is also relevant for the male germ line, where mtDNA mutations can alter sperm motility<sup>25</sup> and hence affect fertility. Notably, at 14.5 d.p.c., female PGCs ( $n = 83$ , mean mtDNA copies = 1,376, s.d. = 601) contained lower amounts of mtDNA than male PGCs ( $n = 43$ , mean mtDNA copies = 2,152, s.d. = 951, two-sample *t*-test  $P < 0.001$ , Fig. 1c), possibly because a stringent bottleneck is more important for the female germ line, with the potential transmission of mutations to subsequent generations. It is also of interest that we observed a range of values for the minimum amount of mtDNA within PGCs (Fig. 1c). This could reflect slight differences in the developmental stage or asymmetric compartmentalization of mtDNA during development. Subtle differences in the parameters governing the genetic bottleneck, such as the timing of the initiation of mtDNA replication, provide an explanation for the apparent difference in bottleneck size seen in

**Figure 2** Models of the mitochondrial genetic bottleneck. Schematic diagram showing a heteroplasmic fertilized oocyte (top), a model of the mitochondrial genetic bottleneck (middle) and subsequent primary oocytes (bottom). Blue circles, wild-type mtDNA; red circles, mutated mtDNA. Time scale shown on the left in d.p.c. (a) Single-sampling model. A single random sample of mtDNA molecules is assumed to repopulate each primary oocyte. (b) Multiple-sampling model. Using an adaptation of the population genetic model of Sewall Wright<sup>16</sup>, this approach assumes that an identical moderate genetic bottleneck is present over multiple cell divisions. In mice,  $G = 15$ , which is the number of divisions required to produce the 25,791 primary oocytes present by 13.5 d.p.c.<sup>21</sup> from a single blastomere. (c) Complex biological model based upon the number of cell divisions leading up to the formation of 40 primordial germ cells (PGCs) at 7.25 d.p.c., followed by 9–10 cell divisions required to generate the 25,791 PGCs required to form a full complement of primary oocytes (for details see **Supplementary Fig. 1**).



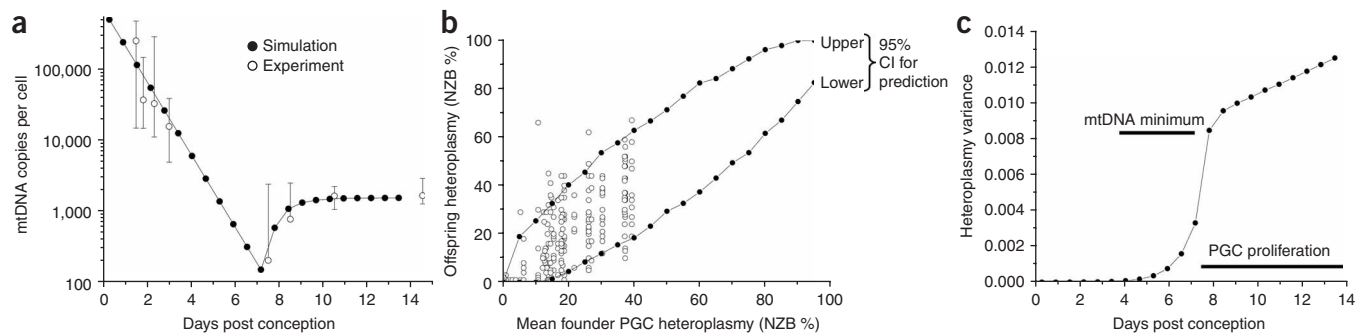


**Figure 3** Modeling the inheritance of mtDNA heteroplasmy in mice. **(a)** Comparison between the simulated amount of mtDNA in each cell (solid circles) and the actual amount measured in preimplantation embryos and primordial germ cells (open circles indicate median, with the range for the laboratory data). **(b)** Comparison of the heteroplasmy values predicted by the biological model with the actual heteroplasmy values in 246 heteroplasmic mice (open circles). The y axis shows the percentage of NZB mtDNA in the offspring and the x axis the estimated percentage of NZB mtDNA in the founding primordial germ cells (PGCs) of the mother. The solid symbols and lines indicate the 95% confidence interval (CI) for the predicted heteroplasmy level using the biological model (**Fig. 2c**). **(c)** Generation of the heteroplasmy variance in the blastomeres and primordial germ cells in a mother with 50% mutated mtDNA.

different human pedigrees transmitting pathogenic mtDNA mutations<sup>26</sup>, with some women having offspring with similar levels of heteroplasmy<sup>3</sup> and others having offspring who are markedly different in this regard<sup>7</sup>.

## METHODS

**Isolation of single embryonic cells.** All animal procedures were performed, under license, in accordance with the UK Home Office Animal Act (1986). C57BL/6J.CBA F<sub>1</sub> female mice were superovulated by sequential intraperitoneal injection of 5 international units (IU) of pregnant mares' serum (PMS) (Sigma-Aldrich) and 7.5 IU of human chorionic gonadotrophin (hCG) (Sigma-Aldrich) 48 h apart. Unfertilized eggs were collected 12 h after hCG injection. One-cell zygotes were collected after successful mating with CBA males 24 h after hCG injection. Single-cell embryos were recovered by flushing the oviducts with prewarmed M2 medium (Sigma-Aldrich) as described<sup>27</sup>. The freshly recovered embryos were transferred to prewarmed M16 media (Sigma-Aldrich) and maintained at 37 °C in a humidified atmosphere containing 5% CO<sub>2</sub> until they reached the cleavage stage required. Embryos were transferred to sterile PCR tubes and lysed for 16 h in 50 mM Tris-HCl, pH 8.5, with 0.5% Tween 20 and 100 µg proteinase K, at 55 °C, followed by heat inactivation at 95 °C for 10 min, a protocol shown previously to maximize the mtDNA yield. Where individual blastomeres were required, the zona pellucida of embryos was removed with acid Tyrode's solution (pH 3.5). The zona-free embryos were then incubated for 10–20 min at 37 °C in calcium- and magnesium-free phosphate-buffered saline. Individual blastomeres were obtained by repeatedly passing the zona-free embryos through a micropipette and lysed as described previously.

**Quantification of mtDNA copy number.** Absolute quantification of mtDNA copy number was performed by real-time PCR using iQSybr Green on the Bio-Rad ICycler to a target template spanning nt12789–nt12876 of the *MTND5* gene. Absolute quantification was performed by the standard curve method. A PCR-generated template was created spanning the mitochondrial genome between nt12705 and nt13834. The template was purified by gel extraction (Qiagen), quantified by UV absorbance at 260 nm and serially diluted to generate a standard curve for quantification of mtDNA content in samples. All samples and standards were measured in triplicate. Before studying mouse embryos, we compared three different real-time PCR assays directed at different regions of the mitochondrial genome: ND5 (nt12789–nt12876), ND4 (nt11031–11174), and ND1 (nt2751–nt3709). The results obtained from each assay were tightly correlated ( $r^2 > 0.99$ ) over a wide range of mtDNA concentrations, encompassing the values obtained in subsequent single cell studies (**Supplementary Fig. 3** online). We arbitrarily chose the ND5 assay for subsequent experiments.

**Isolation of primordial germ cells.** Traditionally, primordial germ cells (PGCs) have been identified by their characteristic tissue nonspecific alkaline phosphatase (TNAP) staining<sup>20</sup>. However, TNAP is also present in somatic cells that surround the PGCs, and the TNAP staining procedure inhibits the mtDNA quantification assay. We initially studied unfixed TNAP-stained cryostat sections, capturing PGCs by laser microdissection. However, copy number measurements were highly variable, partly because the reaction product inhibited the real-time PCR reaction and partly because the reaction product diffused out of the PGCs into the adjacent tissue, making the identification of PGCs difficult. All postimplantation studies were therefore carried out in *Stella-GFP* transgenic mice to allow unambiguous detection of the PGCs.

C57BL/6J.CBA F<sub>1</sub> females were mated with *Stella-GFP* BAC-homozygous C57BL/6J.CBA males<sup>15</sup>. Noon on the day of vaginal plug detection was designated 0.5 d.p.c. *Stella-GFP* heterozygous embryos were collected at 7.5 d.p.c., 8.5 d.p.c., 10.5 d.p.c. and 14.5 d.p.c. in Dulbecco's minimal essential medium (DMEM, Invitrogen) supplemented with 7.5% FCS and 10 mM HEPES. The posterior parts of the 7.5-d.p.c. and 8.5-d.p.c. embryos and the gonadal ridges of 10.5-d.p.c. and 14.5-d.p.c. embryos were dissected using tungsten needles, pooled by age and trypsinized for 15 min at 37 °C. Morphological gender typing was possible after 12.5 d.p.c. The tissue was resuspended under the microscope using an equal volume of FCS and centrifuged for 3 min at 2,000g, and the final pellet was resuspended in DMEM with 7.5% FCS and 10 mM HEPES. Samples were kept on ice until FACS sorting.

Single PGCs and sets of 5, 10, 50 and 100 PGCs were unidirectionally sorted into single wells of a 96-well plate using a BD FACSAria (Becton Dickinson). GFP was detected using a 100-mW sapphire laser and GFP-positive PGCs sorted at 20 p.s.i. using a 100-µm nozzle at a sort rate of 2,000 events per second. Instrument sensitivity was proved stable between sorts by internal QC procedures. Plates were stored at –80 °C until required. PGCs were lysed and mtDNA content quantified as described above.

**Generation of heteroplasmic mice.** Initially mouse strains were backcrossed to maximize reproductive performance and maintain a pure C57BL/6J or NZB mtDNA genotype. Thus, C57BL/6J.C3H F<sub>1</sub> females were crossed with C57BL/6J.C3H F<sub>1</sub> males, and the resulting F<sub>2</sub> females backcrossed with C57BL/6J.C3H F<sub>1</sub> males. The F<sub>3</sub> mice therefore had a C57BL/6J mtDNA genotype on a mixed C57BL/6J and C3H nuclear background. These were designated 'C57mt' mice. Likewise, NZB.NZW F<sub>1</sub> females (obtained from the Jackson Laboratory) were crossed with C57BL/6J.C3H F<sub>1</sub> males, and the F<sub>2</sub> females backcrossed with C57BL/6J.C3H F<sub>1</sub> males. The F<sub>3</sub> mice had a NZB mtDNA genotype on a mixed C57BL/6J, C3H and NZB nuclear background and were designated as 'NZBmt' mice.

Fertilized oocytes were obtained from both C57mt and NZBmt mice using standard techniques. Approximately 10–30% of cytoplasm was removed by



micropipette from a C57mt oocyte, and an equivalent amount of cytoplasm was removed from an NZBmt oocyte. The cytoplasm removed from the C57mt oocyte was microinjected under the zona pellucida of the NZBmt oocyte<sup>28,29</sup> and vice versa. The donor and recipient cytoplasts were fused by electrofusion, and oocytes were implanted into a pseudo-pregnant dam. Seven founder mice (four females and three males) were obtained from the transfer of cytoplasm from an NZBmt oocyte to a C57mt oocyte. Four founder mice (three females and one male) were obtained from the transfer of cytoplasm from a C57mt oocyte to an NZBmt oocyte. The C57mt founder females were mated to C57BL/6J males to breed heteroplasmic mice with a C57mt nuclear background. The NZBmt founder females were caged with NZB males, but pups were not obtained from any of these females.

**Quantification of levels of heteroplasmy.** The transmission of heteroplasmy between a dam and her pups was investigated by measuring the percentage levels of NZB mtDNA in tail biopsies at weaning. There was no difference in the percentage level of NZB mtDNA at this stage between different tissues. Tail biopsies were taken by removing approximately 1 cm of tail with a sterile scalpel blade under anesthesia. Genomic DNA was extracted by incubating in 1.5 ml Salting Out Lysis Buffer (10 mM Tris-Cl, pH 7.5; 0.4 M NaCl; 2 mM EDTA), 200  $\mu$ l 20% SDS and 250  $\mu$ l of 5 mg/ml proteinase K (Boehringer Mannheim) for 16 h at 50 °C. Protein was extracted using 25:24:1 phenol/chloroform/isoamyl alcohol and then 24:1 chloroform/isoamyl alcohol. An ethanol precipitation was performed on each sample and the DNA was redissolved in sterile distilled, deionized water. The concentration was quantified by measuring the absorbance at 260 nm. PCRs were performed in 50- $\mu$ l reaction volumes containing 1 $\times$  *Taq* Polymerase Reaction Buffer (Boehringer Mannheim), 0.2 mM dNTPs, 0.5  $\mu$ g each of primers m3558-F and m3940-R (see **Supplementary Table 2** online for primer sequences), 50 ng of genomic DNA and 2.5 units of *Taq* Polymerase (Boehringer Mannheim). The reactions were overlaid with 100  $\mu$ l of paraffin oil and amplified for 25 cycles of 95 °C for 1 min, 51 °C for 1 min and 72 °C for 1 min on a Corbett Research FTS-320 Thermal Sequencer. The PCR was paused at the start of the 25th cycle (at 95 °C), 10  $\mu$ Ci of [ $\alpha$ -<sup>32</sup>P]dCTP was added to each reaction, and the 25th cycle was then completed.

Restriction endonuclease digests were performed in 20- $\mu$ l volumes containing 15  $\mu$ l of PCR volume, 1 $\times$  Buffer L (Boehringer Mannheim) and 1.5 units of *RsaI* restriction endonuclease (Boehringer Mannheim). The digests were incubated at 37 °C for 16 h, and 5  $\mu$ l of 10% gel loading buffer was added to stop each reaction. *RsaI* cuts C57BL/6J mtDNA twice to yield fragments of 218 base pairs (bp), 132 bp and 32 bp, and cuts NZB mtDNA once to yield fragments of 350 bp and 32 bp. Undigested mtDNA can be detected by the presence of a 382-bp fragment.

A 10- $\mu$ l aliquot of each sample was electrophoresed through an 8% non-denaturing polyacrylamide gel for 2 h at 50 V. The gel was soaked in fixing solution (10% glacial acetic acid and 10% methanol) for 10 min, placed on blotting paper (Schleicher & Schuell) and dried at 80 °C for 2 h. The dried gels were placed against a phosphorimager screen (Molecular Dynamics) for 2 d, and the screen was scanned using a Storm PhosphorImager (Molecular Dynamics). The intensities for the 350-bp (NZB mtDNA) and the 218-bp and 132-bp (C57BL/6J mtDNA) fragments were quantified using ImageQuant software (Molecular Dynamics) and their heteroplasmy levels quantified.

**Modeling.** Previous studies<sup>8</sup> used an adapted population genetic model<sup>16</sup> to model the random segregation of mtDNA genotypes over a number of cell divisions, where the number of copies of mtDNA remained constant over the cell generations. Our experimental observations of the mtDNA copy number per cell show that the copy number is not constant. To account for the varying mtDNA content of different germline precursors, we simulated the process of mtDNA segregation directly, based on the population genetic principles of random segregation. However, by directly simulating the process, we were able to alter the number of mtDNA copies at each stage of PGC development, reflecting our laboratory observations.

The embryogenesis simulation began with a single cell, the fertilized oocyte, that underwent a series of rapid cell divisions, during which mtDNA replication did not occur. Cell divisions were set to occur at constant intervals of 15 h, in agreement with experimental values (**Supplementary Fig. 1**). The existing

mtDNA molecules were simply partitioned randomly between the two daughter cells at each cell division, and the mtDNA content per cell therefore dropped exponentially during this phase, to a minimum of  $314 \pm 24$  in accordance with the experimental values (**Table 2**). To generate the >200,000 mtDNAs we observed in a mature oocyte (**Table 1**), mtDNA replication must resume at some point during oocyte development and markedly increase the number of copies per cell over a sustained period of exponential PGC proliferation<sup>20,21</sup>. In our simulation, mtDNA replication was initiated at 7.5 d.p.c. This value was chosen to simulate the median number of mtDNA molecules that we measured in 7.5-d.p.c. PGCs. It should be noted that there was considerable variation in the measured amount of mtDNA within single PGCs at this time point, with a mean value that was greater than the median. The observed variation in copy number at this point was not incorporated into the model.

At this stage, after ten cell divisions, the total number of cells was 1,024. We modeled the development of a specialized PGC line at this stage by randomly choosing 40 of these simulated cells, while discarding the others from the simulation. These 40 cells continued to divide with a period of 15 h. We followed this process over a further 10 cell divisions, to a final population at 13.4 d.p.c.

The initial cell in the simulation had a heteroplasmic mtDNA population, set at 50% mutant and 50% wild type. The random processes of distribution of wild-type and mutant mtDNA to daughter cells, mtDNA degradation and mtDNA replication all caused the heteroplasmy level in each simulated cell to drift over time, generating a heteroplasmy variance across all of the simulated cells. During the first phase of embryogenesis, while the mtDNA copy number per cell was still relatively high, very little heteroplasmy variance was generated. As the mtDNA copy number per cell fell to a few hundred copies, heteroplasmy variance began to rise. After mtDNA replication began, and the PGC line was formed, mtDNA copy number per cell rose again, to approximately 1,500 per cell. The heteroplasmy variance slowed its rate of increase, but it continued to increase at a steady rate as long as the PGC cell divisions continue at a rapid pace.

We used the actual measurements of mtDNA content within single cells (**Tables 1 and 2**) to simulate the formation of PGCs in mothers with different heteroplasmy values ranging from 1% to 100% (**Fig. 3c**). Each simulation was carried out ten times, resulting in a total of 204,800 cells, allowing us to determine the 95% CI for the heteroplasmy value in individual PGCs for that mother. The upper and lower 95% CI plotted on **Figure 3c** (solid circles) show the likely range of heteroplasmy values across the whole range (solid lines). At birth there was no difference in the proportion of NZB mtDNA between different tissues, but postnatal segregation of mtDNA genotypes led to significant differences between the tail mtDNA and other tissues in adult mice (S.L. White, W. Hutchison, D.R. Thorburn, V.A. Collins, K. Fowler & H.-H.M.D., unpublished data and ref. 30). Given that the transmission of NZB heteroplasmy is determined by random genetic drift<sup>8</sup>, with an equal likelihood of an increase or decrease in the proportion of mtDNA, we estimated the percentage NZB in the maternal primordial germ cell founders as the mean level of heteroplasmy from the offspring at birth.

*Note: Supplementary information is available on the Nature Genetics website.*

#### ACKNOWLEDGMENTS

P.F.C. is a Wellcome Trust Senior Fellow in Clinical Science and also receives funding from the United Mitochondrial Diseases Foundation and from the EU FP6 program EUMitocombat and MITOCIRCLE. H.-H.M.D. is a National Health and Medical Research Council (Australia) Principal Research Fellow, and his affiliations are with The Murdoch Children's Research Institute and the Department of Paediatrics (University of Melbourne), Royal Children's Hospital, Melbourne, Australia. We thank I. Dimmick for his assistance with the flow cytometry, D. Turnbull and B. Lightowlers for discussions, A. McLaren for her expertise on the cell dynamics of mouse development, and M. Azim Surani for providing the *Stella-GFP* mice. We also thank D. Thorburn for discussions and advice while studying the heteroplasmic mice, and both W. Hutchinson and S. White for experimental work on the heteroplasmic mice.

#### AUTHOR CONTRIBUTIONS

This laboratory study was designed by P.F.C. and L.M.C. and carried out by L.M.C. The *in silico* modeling was designed by D.C.S., programmed by H.K.R. and carried out by D.C.S., H.K.R. and P.W. *GFP-Stella* mice were produced in the

laboratory of M. Azim Surani by S.C.d.S.L. H.-H.M.D. designed and supervised the heteroplasmic mouse work. J.R.M. generated the heteroplasmic mice.

Published online at <http://www.nature.com/naturegenetics>

Reprints and permissions information is available online at <http://npg.nature.com/reprintsandpermissions>

1. Holt, I.J., Miller, D.H. & Harding, A.E. Genetic heterogeneity and mitochondrial DNA heteroplasmy in Leber's hereditary optic neuropathy. *J. Med. Genet.* **26**, 739–743 (1989).
2. Bolhuis, P.A. *et al.* Rapid shift on genotype of human mitochondrial DNA in a family with Leber's hereditary optic neuropathy. *Biochem. Biophys. Res. Commun.* **170**, 994–997 (1990).
3. Viikari, J., Savontaus, M.L. & Nikoskelainen, E.K. Segregation of mitochondrial genomes in a heteroplasmic lineage with Leber hereditary optic neuropathy. *Am. J. Hum. Genet.* **47**, 95–100 (1990).
4. Larsson, N.G. *et al.* Segregation and manifestations of the mtDNA tRNA(Lys) A→G(8344) mutation of myoclonus epilepsy and ragged-red fibers (MERRF) syndrome. *Am. J. Hum. Genet.* **51**, 1201–1212 (1992).
5. Upholt, W.B. & Dawid, I.B. Mapping of mitochondrial DNA of individual sheep and goats: rapid evolution in the D loop region. *Cell* **11**, 571–583 (1977).
6. Olivo, P.D., Van de Walle, M.J., Laipis, P.J. & Hauswirth, W.W. Nucleotide sequence evidence for rapid genotypic shifts in the bovine mitochondrial DNA D-loop. *Nature* **306**, 400–402 (1983).
7. Blok, R.B., Gook, D.A., Thorburn, D.R. & Dahl, H.H. Skewed segregation of the mtDNA nt 8993 (T to G) mutation in human oocytes. *Am. J. Hum. Genet.* **60**, 1495–1501 (1997).
8. Jenuth, J.P., Peterson, A.C., Fu, K. & Shoubridge, E.A. Random genetic drift in the female germ line explains the rapid segregation of mammalian mitochondrial DNA. *Nat. Genet.* **14**, 146–151 (1996).
9. Chinnery, P.F. *et al.* The inheritance of mtDNA heteroplasmy: random drift, selection or both? *Trends Genet.* **16**, 500–505 (2000).
10. Brown, D.T., Samuels, D.C., Michael, E.M., Turnbull, D.M. & Chinnery, P.F. Random genetic drift determines the level of mutant mitochondrial DNA in human primary oocytes. *Am. J. Hum. Genet.* **68**, 533–536 (2001).
11. Piko, L. & Taylor, K.D. Amounts of mitochondrial DNA and abundance of some mitochondrial gene transcripts in early mouse embryos. *Dev. Biol.* **123**, 364–374 (1987).
12. Steuerwald, N. *et al.* Quantification of mtDNA in single oocytes, polar bodies and subcellular components by real-time rapid cycle fluorescence monitored PCR. *Zygote* **8**, 209–215 (2000).
13. Larsson, N.G. *et al.* Mitochondrial transcription factor A is necessary for mtDNA maintenance and embryogenesis in mice. *Nat. Genet.* **18**, 231–236 (1998).
14. McLaren, A. & Lawson, K.A. How is the mouse germ-cell lineage established? *Differentiation* **73**, 435–437 (2005).
15. Payer, B. *et al.* Generation of stella-GFP transgenic mice: a novel tool to study germ cell development. *Genesis* **44**, 75–83 (2006).
16. Wright, S. *Evolution and the Genetics of Populations* (University of Chicago Press, Chicago, 1969).
17. Bendall, K.E., Macaulay, V.A., Baker, J.R. & Sykes, B.C. Heteroplasmic point mutations in the human mtDNA control region. *Am. J. Hum. Genet.* **59**, 1276–1287 (1996).
18. Poulton, J., Macaulay, V. & Marchington, D.R. Mitochondrial genetics '98: Is the bottleneck cracked? *Am. J. Hum. Genet.* **62**, 752–757 (1998).
19. Streffer, C., Van Beuningen, D., Mollis, M., Zamboglou, N. & Schultz, S. Kinetics of cell proliferation in the pre-implanted mouse embryo *in vivo* and *in vitro*. *Cell Tissue Kinet.* **13**, 135–143 (1980).
20. Ginsburg, M., Snow, M.H.L. & McLaren, A. Primordial germ cells in the mouse embryo during gastrulation. *Development* **110**, 521–528 (1990).
21. Tam, P.P.L. & Snow, M.H.L. Proliferation and migration of primordial germ cells during compensatory growth in mouse embryos. *J. Embryol. Exp. Morphol.* **64**, 133–147 (1981).
22. Downs, K.M. & Davies, T. Staging of gastrulating mouse embryos by morphological landmarks in the dissecting microscope. *Development* **118**, 1255–1266 (1993).
23. Cao, L. *et al.* The mitochondrial bottleneck occurs without reduction of mtDNA content in female mouse germ cells. *Nat. Genet.* **39**, 386–390 (2007).
24. Bergstrom, C.T. & Pritchard, J. Germline bottlenecks and the evolutionary maintenance of mitochondrial genomes. *Genetics* **149**, 2135–2146 (1998).
25. Spiropoulos, J., Turnbull, D.M. & Chinnery, P.F. Can mitochondrial DNA mutations cause sperm dysfunction? *Mol. Hum. Reprod.* **8**, 719–721 (2002).
26. Howell, N. *et al.* Mitochondrial gene segregation in mammals: is the bottleneck always narrow? *Hum. Genet.* **90**, 117–120 (1992).
27. Hogan, B., Beddington, R., Constantini, F. & Lacy, E. *Manipulating the Mouse Embryo* (Cold Spring Harbor Laboratory Press, Cold Spring Harbor, New York, USA, 1994).
28. McGrath, J. & Solter, D. Nuclear transplantation in the mouse embryo by microsurgery and cell fusion. *Science* **220**, 1300–1302 (1983).
29. Mann, J.R., Gadi, I., Harbison, M.L., Abbondanzo, S.J. & Stewart, C.L. Androgenetic mouse embryonic stem cells are pluripotent and cause skeletal defects in chimeras: implications for genetic imprinting. *Cell* **62**, 251–260 (1990).
30. Jenuth, J.P., Peterson, A.C. & Shoubridge, E.A. Tissue-specific selection for different mtDNA genotypes in heteroplasmic mice. *Nat. Genet.* **16**, 93–95 (1997).